Numerical simulation of angular structure of the near-horizon sky brightness in ground-based observations. Part 2. The aerosol-gas atmosphere

T.B. Zhuravleva, I.M. Nasretdinov, S.M. Sakerin, K.M. Firsov, and T.Yu. Chesnokova

Institute of Atmospheric Optics, Siberian Branch of the Russian Academy of Sciences, Tomsk

Received September 19, 2003

An efficient algorithm is presented for calculation of the diffuse solar radiation by the conjugate walk method in the spherical aerosol-gas atmosphere. Molecular absorption and spectral instrumental function of photometers are taken into account through parameters of exponential series expansion of the transmission function. Based on the results of computer simulation, it is shown that the neglect of molecular absorption in atmospheric transmission windows leads to errors in radiative calculations, which increase in going from the solar almucantar to the near-horizon sky zone, and under typical atmospheric conditions these errors make from 2 to 40%. The aerosol effect on the diffuse radiation shows itself in the following regularities: the sky brightness decreases almost linearly with the decrease of the single scattering albedo, while its dependence on the aerosol thickness may be nonmonotonic for azimuth viewing angles less than 90°.

Introduction

The refinement of radiative models and development of techniques for solving inverse problems for conditions of the daylight clear sky ground-based observations require an improvement of the radiative calculation algorithms and more thorough consideration of conditions of real experiments, because as the viewing angle approaches the horizon, the effects of atmospheric sphericity, multiple scattering, and molecular absorption manifest themselves to the greatest extent.

In the first part of our paper,[1] the algorithm for calculation of the diffuse radiation by the conjugate walk method was tested, and the effect of atmospheric sphericity and the vertical stratification of the aerosol optical characteristics on the clear-sky brightness field near the horizon was considered *neglecting the absorption by atmospheric gases*. It was shown that (1) at a small aerosol optical thickness and/or large solar zenith angles the neglect of atmospheric sphericity could lead to errors up to 10% in radiative calculations; (2) not only the optical thickness of the atmosphere, but also the aerosol extinction coefficient in the atmospheric surface layer affects the formation of the angular structure of solar radiation near the horizon. Just this is the principal difference between calculations of the sky brightness in the near-horizon area and those for the solar almucantar with the zenith angles less than ~ 80°, where a sufficient accuracy of calculations is achieved by the setting of only the integral characteristic, namely, the atmospheric optical thickness (see, for example, Refs. 2 and 3).

In this paper, we consider the algorithm for the radiative transfer equation (RTE) solution with regard for molecular absorption and spectral instrumental functions of real photometers. Application of the well-known *line-by-line* (LBL) approach accounting for the fine structure of absorption spectra in combination with the Monte Carlo method is very cumbersome and computationally expensive even with modern computers. That is why the molecular absorption is taken into account using the method of exponential series, whose efficiency was demonstrated earlier for a particular problem: simulation of the Earth's surface illumination for the plane model of the atmosphere.[4] We also estimate errors arising in radiative calculations because of neglect of radiation absorption by atmospheric gases and analyze the effect of the aerosol optical characteristics on the near-horizon sky brightness.

1. Method of numerical simulation

The problems of radiative transfer in the scattering and absorbing atmosphere with regard for the fine structure of molecular absorption traditionally involve the use of the LBL method (see, for example, the topical issue of ICRCCM[5]). For numerical solution of RTE based on statistical algorithms in combination with the LBL method, its efficient modification has been developed (for detail, see Ref. 6). The essence of the modification is in the fact that in calculation of the radiation in the spectral interval $\Delta\lambda = (\lambda_1, \lambda_2)$, some additional randomization is introduced: wavelengths $\lambda \in \Delta\lambda$ are chosen randomly, and they form a uniformly distributed sample, which significantly shortens the computations. The disadvantage of this approach is that introduction of the LBL procedure into computer realizations of the Monte Carlo algorithms requires their radical change.

0235-6880/03/12 972-10 $02.00

The ideology of exponential series has been actively used in the last decade along with the LBL method for calculation of molecular absorption. The traditional scheme of the exponential series method is the following[7–10]:

1) mass calculations of transmission functions are carried out for various meteorological situations and observation geometry;

2) the accumulated data array is used to determine the parameters of the transmission function expansion into the exponential series with regard for the fact that the characteristics of molecular absorption depend on the air temperature and pressure.

The use of exponential series ensures rather high accuracy of RTE solution. According to the Ellingson data,[11] for example, the calculation error for the downward longwave radiation fluxes in the cloudless atmosphere is ~0.3%. The undoubted advantage of this approach is that it allows one to separate in time the calculation of molecular absorption characteristics and the numerical simulation of the radiative transfer (Monte Carlo method) in the scattering and absorbing atmosphere. At the same time, its disadvantage is that the efficiency of parameterization of the molecular absorption characteristics strongly depends on the investigator's skills and the choice of basic meteorological profiles. Another difficulty is connected with consideration of spectral instrumental functions of actual devices.

In this paper, the molecular absorption is considered using the modified method of exponential series, which allows avoiding the above problems. The effective transmission function caused by molecular absorption in the spectral interval $\Delta\lambda$ can be presented as

$$T^{\mathrm{G}}_{\Delta\lambda}(m) = \int_{\lambda_1}^{\lambda_2} F(\lambda) I_0(\lambda) T^{\mathrm{G}}(m,\lambda)\,\mathrm{d}\lambda / I_{0,\Delta\lambda},$$
$$I_{0,\Delta\lambda} = \int_{\lambda_1}^{\lambda_2} F(\lambda) I_0(\lambda)\,\mathrm{d}\lambda. \qquad (1)$$

Here $F(\lambda)$ is the instrumental function; $I_0(\lambda)$ is the spectral solar constant;

$$T^{\mathrm{G}}(m,\lambda) = \exp\left(-m\int_0^{H_{\mathrm{atm}}} \kappa_{\mathrm{mol}}(\lambda,h)\,\mathrm{d}h\right)$$

is the monochromatic transmission function in the vertically inhomogeneous Earth's atmosphere; $\kappa_{\mathrm{mol}}(\lambda, h)$ is the molecular absorption coefficient at the wavelength λ and the height h; m is the optical mass in the direction to the Sun; H_{atm} is the top height of the atmosphere. Taking into account the weak selectivity of $I_0(\lambda)$, in most cases for calculation of the effective transmission function it is convenient to use the equation

$$T^{\mathrm{G}}_{\Delta\lambda}(m) = \int_{\lambda_1}^{\lambda_2} F(\lambda) T^{\mathrm{G}}(m,\lambda)\,\mathrm{d}\lambda \Big/ \int_{\lambda_1}^{\lambda_2} F(\lambda)\,\mathrm{d}\lambda.$$

According to the approach from Ref. 4, $T^{\mathrm{G}}_{\Delta\lambda}(m)$ can be converted to the form

$$T^{\mathrm{G}}_{\Delta\lambda}(m) = \int_0^1 \exp\left(-m\int_0^{H_{\mathrm{atm}}} k(g,h)\,\mathrm{d}h\right)\mathrm{d}g =$$
$$= \sum_{i=1}^{N} C_i \exp\left(-m\int_0^{H_{\mathrm{atm}}} k(g_i,h)\,\mathrm{d}h\right), \qquad (2)$$

where $k(g, h)$ is the effective absorption coefficient in the space of cumulative wavelengths g; g_i and C_i are the nodes and coefficients of the Gauss quadrature formulae; $\sum_{i=1}^{N} C_i = 1$. It should be noted that, unlike the fast-oscillating function $\kappa_{\mathrm{mol}}(\lambda, h)$, $k(g, h)$ is a piecewise continuous, monotonically growing function of λ. Just this circumstance allows us, applying the Gauss quadrature formulae to numerical integration over the variable g, to obtain readily a short exponential series in Eq. (2). The effective absorption coefficients $k(g, h)$ are calculated through the inverse function $g(k, h)$:

$$g(k,h) = \int_{\lambda_1}^{\lambda_2} F(\lambda) I_0(\lambda) U(\lambda,h)\,\mathrm{d}\lambda / I_{0,\Delta\lambda},$$
$$U(\lambda,h) = \begin{cases} 1, & \kappa_{\mathrm{mol}}(\lambda,h) \le k, \\ 0, & \kappa_{\mathrm{mol}}(\lambda,h) > k. \end{cases} \qquad (3)$$

Earlier, it was shown[4,6] that in the spectral interval $\Delta\lambda = (\lambda_1, \lambda_2)$ the radiative characteristics (brightness, flux) $Q_{\Delta\lambda}$ can be represented in the form

$$Q_{\Delta\lambda} = \sum_{i=1}^{N} C_i Q_i, \qquad (4)$$

where Q_i is the monochromatic radiation at the cumulative wavelength g_i, $i = 1, \ldots, N$. This means that the calculation of $Q_{\Delta\lambda}$ involves two stages: at the first stage the finite set of effective molecular absorption coefficients $\{k_i(h)\}_{i=1}^{N}$ [$k_i(h) \equiv k(g_i, h)$] is calculated, and at the second stage RTE is solved in some or other way for each set $k_i(h)$, $i = 1, \ldots, N$ (usually $N \sim 5$–10).

To be correct, it should be noted that the considered approach is somewhat behind in speed and accuracy as compared to the effective modification of the LBL method.[6] However, there are many important arguments in its favor. First, the computation time increases insignificantly, because it is proportional to the number of terms in the exponential series, which is short enough. Second, separation in time of calculating the molecular absorption coefficients and solving the RTE allows us to use, with minimal correction, the algorithms and programs developed earlier for calculation of radiation neglecting the gas absorption. Third, spectral peculiarities of the instrumental

function and the solar constant can be easily taken into account.

According to the above-said, for calculation of the diffuse radiation brightness given the coordinates of the observation point r^* and the viewing direction $\omega_k = (\xi, \varphi_k)$, we use the equation

$$B_{\Delta\lambda}\left(r^*, \omega_k\right) = \sum_{i=1}^{N} C_i B_i\left(r^*, \omega_k\right), \qquad (5)$$

where ξ and φ_k are the detector's zenith and azimuth angles, $k = 1, 2, \ldots, N_\varphi$. The monochromatic brightness $B_i(r^*, \omega_k)$, corresponding to the ith set of effective molecular absorption coefficients $k_i(h)$, $i = 1, \ldots, N$, is calculated by the conjugate walk method with regard for the atmospheric sphericity.[1] Note that within the considered spectral range $\Delta\lambda = (\lambda_1, \lambda_2)$ the optical characteristics of aerosol are assumed constant. From here on the index $\Delta\lambda$ of the spectrally integral brightness $B_{\Delta\lambda}$ is omitted for simplicity.

The sky brightness in the cloudless atmosphere was calculated for four spectral ranges: 0.50, 0.87, 1.245, and 2.137 μm with the instrumental functions typical for photometers. The aerosol optical characteristics were chosen according to the WCP recommendations[12] for the continental conditions; in the height range of 0–12 km the exponential profile of the aerosol extinction coefficient was used.[1] The particular values of the aerosol optical thickness τ_{aer} (for two types of aerosol turbidity) and the single scattering albedo Λ_{aer} for different spectral regions are summarized in Table 2 (second and third columns). The detector's zenith angle in the horizon zone was $\xi = 89°$. The main calculations were performed for the solar zenith angles $\xi_\odot = 60–85°$, the azimuth viewing angles $0 \le \varphi \le 180°$, and the surface albedo $A_s = 0.2$, 0.8.

The effective absorption coefficients are calculated with the use of the HITRAN-2000 database [http://www.hitran.com]. The vertical profiles of the temperature, air pressure, and concentrations of atmospheric gases (H_2O, CO_2, O_3, CH_4, and others) were specified according to the AFGL meteorological model for the mid-latitude summer.[13] For these spectral ranges and the solar zenith angle $\xi_\odot = 60°$ the absorption optical thickness $\tau^G_{\Delta\lambda}(m) = -\ln T^G_{\Delta\lambda}(m)$ ranged from 0.02 to 0.07 (Fig. 1).

The error in radiative calculations caused by the transition from the LBL method to the effective absorption coefficients in the inhomogeneous atmosphere for the considered spectral ranges and atmospheric conditions did not exceed 0.3–0.5% (the number of the terms of the series in Eq. (2) was $N = 10$). Since the relative error in the calculation of $B_i(r^*, \omega_k)$, $i = 1, \ldots, N$, usually was within 1%, the errors in calculation of $B_{\Delta\lambda}$ were roughly 1.5%.

2. Effect of the instrumental function

Before going to radiative calculations, consider how important is the effect of the instrumental function $F(\lambda)$, which is largely determined by the filtering bandpass. We estimate the effect of $F(\lambda)$ from the direct radiation calculation, because, as will be shown below, the molecular absorption and, consequently, the instrumental function make at least comparable effects on direct and diffuse radiation.

The direct radiation $I_{\Delta\lambda}$ measured in the spectral range (λ_1, λ_2) is determined by the equation

$$I_{\Delta\lambda} = \int_{\lambda_1}^{\lambda_2} I_0(\lambda) T^A(\lambda) T^G(\lambda, m) F(\lambda)\, d\lambda, \qquad (6)$$

where $T^A(\lambda)$ is the atmospheric transmittance due to molecular scattering and aerosol extinction. Because of the low selectivity of $T^A(\lambda)$ and with regard for Eq. (1), Eq. (6) can be simplified:

$$I_{\Delta\lambda} = I_{0,\Delta\lambda} T^A_{\Delta\lambda,\max} T^G_{\Delta\lambda}(m). \qquad (7)$$

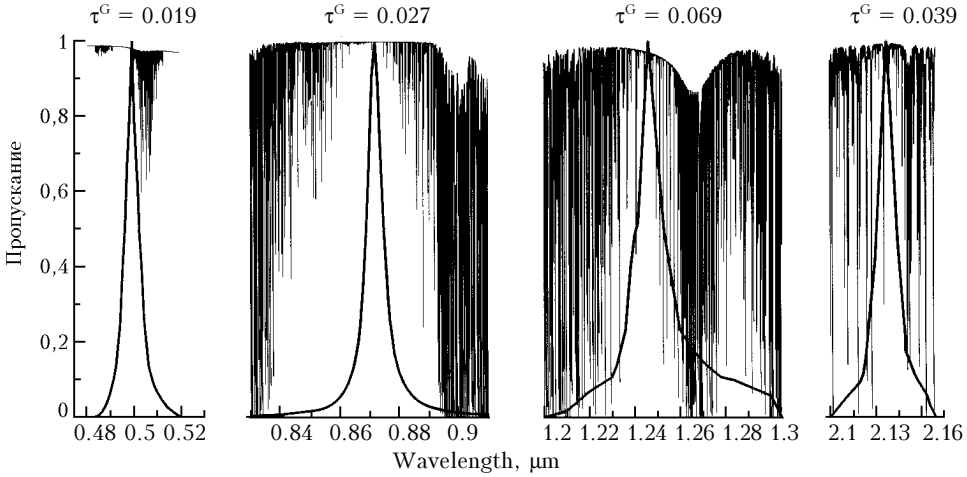

Fig. 1. Absorption spectrum, instrumental functions of interference filters, and absorption optical thickness for the selected spectral ranges ($\xi_\odot = 60°$).

Here $T^{A}_{\Delta\lambda,\max}$ is a $T^{A}(\lambda)$ value at the point corresponding to maximum of the instrumental function.

In the spectral ranges free of noticeable molecular absorption, different approximations of the real instrumental function $F(\lambda)$ are often used (as a rule, in the form of a Π-shaped profile). The presence of absorption bands of atmospheric gases can radically change the situation, and the use of such approximations in place of the actual filtering bandpass can lead to considerable errors in radiative calculations. It should be also kept in mind that the significant contribution to $T^{G}_{\Delta\lambda}$ (and, consequently, $I_{\Delta\lambda}$) can come from radiation absorption in the ranges falling on the filtering bandpass wings, where the accuracy of description of $F(\lambda)$ may be rather low. This rises the question: how necessary is to consider $F(\lambda)$ within the full filtering bandpass (λ_1, λ_2) in calculations of $I_{\Delta\lambda}$ or, perhaps, it is possible to restrict the consideration to some more narrow spectral range (λ_1', λ_2')?

Consider a reference model profile the nearest to the actual one and specified in the spectral interval (λ_1, λ_2). Estimate the error in calculation of $I_{\Delta\lambda}$, which arises as the reference profile is replaced by its "cutoff" version in the range (λ_1', λ_2'). Let δ_T be the relative error in calculation of the effective transmission function:

$$\delta_T = \left(T^{G,cut}_{\Delta\lambda}(m) - T^{G}_{\Delta\lambda}(m)\right) \Big/ T^{G}_{\Delta\lambda}(m), \qquad (8)$$

where

$$T^{G,cut}_{\Delta\lambda}(m) = \int_{\lambda_1'}^{\lambda_2'} T^{G}(\lambda, m) F(\lambda) I_0(\lambda) d\lambda \Big/ \int_{\lambda_1'}^{\lambda_2'} F(\lambda) I_0(\lambda) d\lambda.$$

The obvious consequence from Eq. (8) is the following equation:

$$T^{G,cut}_{\Delta\lambda}(m) = T^{G}_{\Delta\lambda}(m)(1 + \delta_T). \qquad (9)$$

Then, based on Eq. (7) the error in calculation of $I_{\Delta\lambda}$

$$\delta_I = \left(T^{G,cut}_{\Delta\lambda}(m) \int_{\lambda_1'}^{\lambda_2'} F(\lambda) I_0(\lambda) d\lambda - T^{G}_{\Delta\lambda}(m) I_{0,\Delta\lambda} \right) \Big/ \left(T^{G}_{\Delta\lambda}(m) I_{0,\Delta\lambda} \right)$$

can be transformed, with regard for Eq. (10), to the form

$$\delta_I = (1 + \delta_T) \int_{\lambda_1'}^{\lambda_2'} F(\lambda) I_0(\lambda) d\lambda / I_{0,\Delta\lambda} - 1. \qquad (11)$$

Hence, the accuracy of radiative calculations depends on the accuracy of calculation of $T^{G}_{\Delta\lambda}$, and for the "cutoff" true filtering bandpass $\delta_I \le \delta_T$.

In case that some approximation $F_1(\lambda)$ is used in place of the actual instrumental function $F(\lambda)$, we obtain a relation similar to Eq. (11) to estimate the error in calculating $I_{\Delta\lambda}$. In this case, the value of δ_I is affected not only by δ_T, but also, to some or other extent, by the ratio of the functions $F(\lambda)I_0(\lambda)$ and $F_1(\lambda)I_0(\lambda)$ integrated over the appropriate spectral ranges.

Estimate relative calculation errors of the effective transmission function, which follow from different approximations of $F(\lambda)$ and restriction of the interval (λ_1, λ_2), using, as an example, the instrumental function, typical of an interference filter, in 1.245 μm spectral range for the following situations (Table 1):

1) reference filtering bandpass in the interval (λ_1, λ_2) with a halfwidth $\Delta\lambda_{0.5} \approx 12$ nm (full width at half-maximum);

2) Π-shaped band profile of ~ $\Delta\lambda_{0.5}$ width;

3) Gauss profile coinciding with the actual one in the central part;

4) reference profile with restricted wings $(\lambda_2' - \lambda_1') \approx 5\Delta\lambda_{0.5}$;

5) reference profile with restricted wings $(\lambda_2'' - \lambda_1'') \approx 8\Delta\lambda_{0.5}$.

Table 1. Function $T^{G}_{\Delta\lambda}$ and optical thickness $\tau^{G}_{\Delta\lambda}$ for different $F(\lambda)$ at $\xi_{\odot} = 60°$ (mid-latitude summer)

Characteristic	Instrumental function $F(\lambda)$				
	1	2	3	4	5
$T^{G}_{\Delta\lambda}$	0.9154	0.9673	0.9645	0.9285	0.9251
$(\Delta T^{G}_{\Delta\lambda} / T^{G,1}_{\Delta\lambda})$, %	–	5.7	5.4	1.4	1.06
$\tau^{G}_{\Delta\lambda} = -\ln T^{G}_{\Delta\lambda}$	0.0884	0.0333	0.0362	0.0742	0.0778

Note: $T^{G,1}_{\Delta\lambda}$ is the transmission function for the reference profile of the filtering bandpass.

From the results presented it follows that the use of the simplified instrumental functions $F(\lambda)$ like the Π-shaped and Gauss profiles in IR atmospheric transmission windows leads to higher than ≈ 5%-errors in calculation of the effective transmission function. The calculations made for the 4th and 5th profiles allow us to estimate the contribution of the filtering bandpass wings to $T^{G}_{\Delta\lambda}(m)$. They show that to obtain the acceptable agreement between the calculations and the data of actual measurements, it is necessary to take into account $F(\lambda)$ in a rather wide spectral range $(\lambda_2' - \lambda_1') > 10\Delta\lambda_{0.5}$.

3. Effect of molecular absorption

As it was noted above, molecular absorption is often assumed negligible in calculations of diffuse radiation. This assumption is justified for atmospheric transmission windows in the visible spectral range and zenith viewing angles up to 70–80°, but it is not

so obvious in the near-IR region and at $\xi > 80°$, when the role of multiple scattering overburdened by absorption increases. In this connection, it is interesting to estimate the effect of atmospheric absorption on the sky brightness not only for sensing in direction to horizon, but also for a well-known problem of the solar almucantar at large zenith angles.

The effect of molecular absorption on brightness calculations was assessed in the form of absolute (Δ) and relative (δ) errors:

$$\Delta = B^{A} - B^{AG}, \quad \delta = 100\%(B^{A} - B^{AG}) / B^{AG}. \quad (12)$$

Here the superscripts AG and A stand for calculations made with allowance for molecular absorption and neglecting it, respectively. For completeness of the analysis, we additionally considered the errors in the brightness components caused by single (subscript 0) and multiple (subscript m) scattering.

It is clear from general reasoning that the errors (12) must increase as the molecular absorption and the number of interaction events increase, that is, with increase of the absorption optical thickness and zenith viewing angle. This can be most easily shown by the example of the brightness component caused by single scattering. Using the initial equations from Refs. 14 and 15 for the vertically homogeneous plane-parallel atmosphere, it is possible to represent the single scattered radiation in the solar almucantar as follows:

for the aerosol atmosphere

$$B^{A}_{0,alm}(\theta) = I_{0,\Delta\lambda}[\tau_{aer}\Lambda_{aer}g_{aer}(\theta) + \tau_{R}g_{R}(\theta)]\exp[-(\tau_{aer} + \tau_{R})m]; \quad (13a)$$

for the aerosol-gas atmosphere

$$B^{AG}_{0,alm}(\theta) = I_{0,\Delta\lambda}T^{G}_{\Delta\lambda}(m)[\tau_{aer}\Lambda_{aer}g_{aer}(\theta) + \tau_{R}g_{R}(\theta)]\exp[-(\tau_{aer} + \tau_{R})m], \quad (13b)$$

where $m \approx \sec\xi_{\odot}$ for $\xi_{\odot} \le 80°$; τ_{R} is the optical thickness of molecular (Rayleigh) scattering; $g_{aer}(\theta)$ and $g_{R}(\theta)$ are the aerosol and Rayleigh scattering phase functions; θ is the scattering angle related to the azimuth angle φ as $\cos\theta = \sin\xi\sin\xi_{\odot}\cos\varphi + \cos\xi\cos\xi_{\odot}$.

Similar equations can also be written for the geometry of horizontal observation:

$$B^{A}_{0,h}(\theta) = I_{0,\Delta\lambda}\frac{\tau_{aer}\Lambda_{aer}g_{aer}(\theta) + \tau_{R}g_{R}(\theta)}{\tau_{aer} + \tau_{R}} \times \exp[-(\tau_{aer} + \tau_{R})m], \quad (14a)$$

$$B^{AG}_{0,h}(\theta) = I_{0,\Delta\lambda}T^{G}_{\Delta\lambda}(m)\frac{\tau_{aer}\Lambda_{aer}g_{aer}(\theta) + \tau_{R}g_{R}(\theta)}{\tau_{aer} + \tau_{R} + \tau^{G}_{\Delta\lambda}(m)} \times \exp[-(\tau_{aer} + \tau_{R})m]. \quad (14b)$$

From Eqs. (13) and (14) we can readily obtain the equations for the errors arising due to neglect of absorption:

$$\delta_{0,alm} = [T^{G}_{\Delta\lambda}(m)]^{-1} - 1,$$

in atmospheric transmission windows ($T^{G}_{\Delta\lambda} \to 1$)

$$\delta_{0,alm} \approx \tau^{G}_{\Delta\lambda}(m), \quad (15a)$$

$$\delta_{0,h} = [T^{G}_{\Delta\lambda}(m)]^{-1}\left[1 + \frac{\tau^{G}_{\Delta\lambda}}{\tau_{aer} + \tau_{R}}\right] - 1. \quad (15b)$$

(The equations for absolute errors have a similar form, since $\Delta = \delta B^{AG}$).

The obtained equations show that, as for the direct radiation, the neglect of absorption by atmospheric gases leads to overestimated radiation, and the difference is determined by the slant absorption optical thickness $\tau^{G}_{\Delta\lambda}(m)$. In the geometry of near-horizon observation, Eq. (15b), the errors increase as the optical thickness ($\tau_{aer} + \tau_{R}$) decreases; and with all other optical characteristics being the same, their values are larger than those for the solar almucantar: $\delta_{0,h} > \delta_{0,alm}$. The foregoing approximate estimates concern the dependence of only the single scattering component of δ_{0} on the main factor — molecular absorption. The effects of other conditions on Δ and δ can be found from numerical simulation for the vertically inhomogeneous spherical atmosphere.

Figure 2 depicts the results of calculation of $B^{A}(\varphi)$, $B^{AG}(\varphi)$ and the difference $\Delta(\varphi)$ for two values of the aerosol thickness and the surface albedo. Both for the solar almucantar and sensing in the horizontal direction, the angular behavior of $\Delta(\varphi)$ qualitatively copies the dependence of $B^{AG}(\varphi)$ with maximum values near the forward scattering angles. The increase of A_{s} leads to some growth of absolute errors because of the increasing number of scattering and absorption events, while the relative errors δ vary insignificantly.

The effect of the aerosol optical thickness on Δ depends on the experiment geometry. As follows from the data summarized for various conditions and spectral channels (Table 2, Fig. 2), for solar almucantar the growth of τ_{aer} leads to the increase of the absolute difference Δ_{alm}, while δ_{alm} remains almost unchanged. The dependence of Δ_{h} and δ_{h} on τ_{aer} near the horizon is not simple and is determined by a number of factors, in particular, by the complex influence of the atmospheric sphericity at variation of τ_{aer} and the solar zenith angle.

The errors in different spectral channels are distributed according to the absorption optical thickness $\tau^{G}_{\Delta\lambda}(m)$ value. It follows from Fig. 3 that for the solar almucantar (curves *1*, *2*) the dependence $\delta_{alm} = f(\tau^{G}_{\Delta\lambda})$ is close to linear and almost coincides with the approximate single scattering Eq. (15a). Near the horizon, the dependence of δ_{h} on $\tau^{G}_{\Delta\lambda}(m)$ has a more complex character (curves *3–5*), since δ_{h} also depends on τ_{aer} and $\xi_{\odot}$ [see the approximation (15b)]. Nevertheless, a general tendency is that δ_{h} grows as the molecular absorption and zenith angle $\xi_{\odot}$ increase.

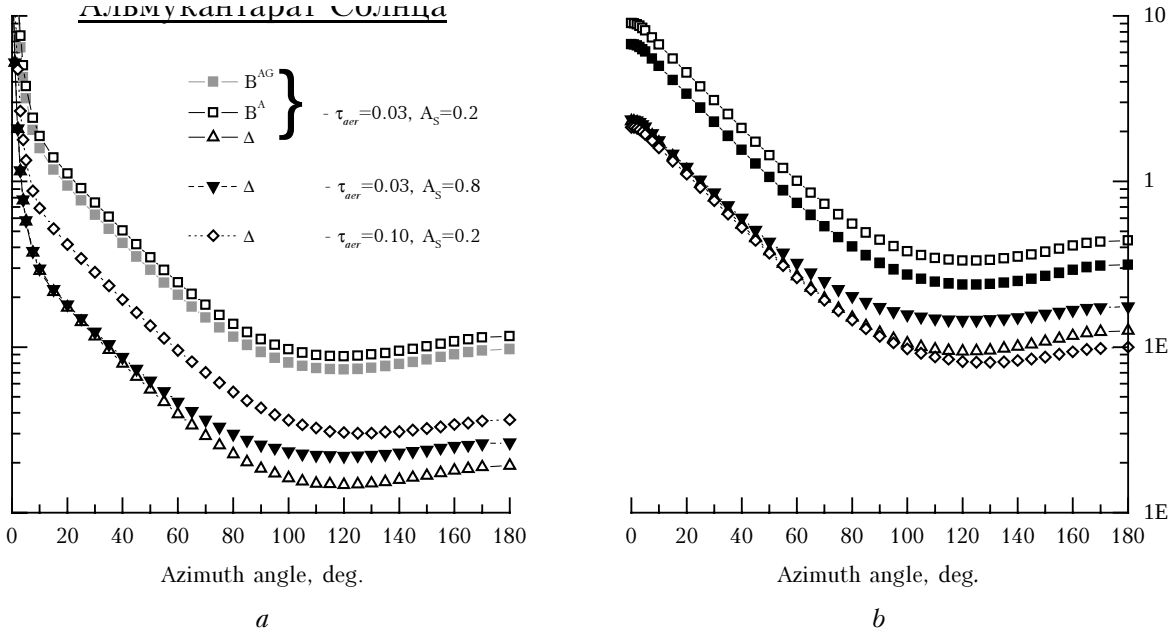

Fig. 2. Angular dependence of B^{AG}, B^{A}, and Δ in the solar almucantar (*a*) and near the horizon (*b*) (λ = 1.245 μm, $\xi_\odot$ = 80°).

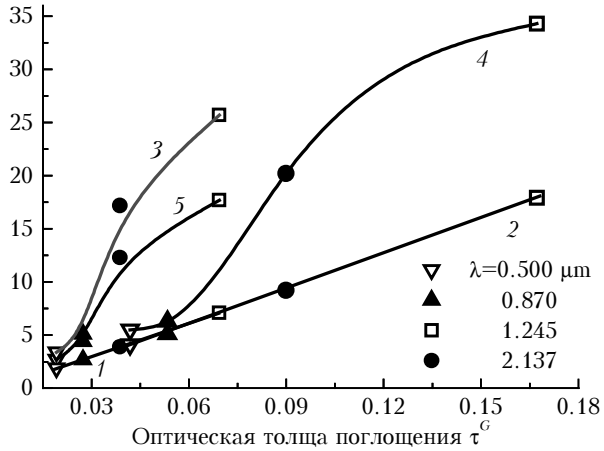

Fig. 3. Effect of the molecular absorption neglect on the sky brightness depending on $\tau^{G}_{\Delta\lambda}(m)$ for $A_s = 0.2$, $\tau_{aer} = 0.03$, $\varphi = 0°$: $\delta_{alm}(\xi_\odot = 60°)$ (*1*); $\delta_{alm}(\xi_\odot = 80°)$ (*2*); $\delta_h(\xi_\odot = 60°)$ (*3*); $\delta_h(\xi_\odot = 80°)$ (*4*); $\delta_h(\xi_\odot = 80°, \tau_{aer} = 0.1)$ (*5*).

Note that in a wide range of input parameters of the problem for all spectral ranges (see Table 2), the inequality $\delta_h > \delta_{alm}$ is fulfilled, and the total range of errors $\delta \approx 2$–40%: the minimal values take place in the 0.5 μm spectral channel for the solar almucantar ($\xi_\odot = \xi = 60°$), while the maximal ones are observed in the 1.245 μm channel near the horizon ($\xi_\odot = 80°$, $\xi = 89°$).

In conclusion of this section, consider the dependence of δ and relative errors of single (δ_0) and multiple (δ_m) scattering on the azimuth angle φ (Fig. 4). For the solar almucantar, regardless of τ_{aer} and other conditions, the single scattering component $\delta_{0,alm}(\varphi) \approx$ const, while the multiple scattering component $\delta_{m,\,alm}(\varphi)$ increases monotonically with the growth of φ (in the channels with weak absorption this effect almost does not show itself). For the horizontal direction, the angular behavior of δ_h, $\delta_{0,h}$, and $\delta_{m,h}$ at a small aerosol optical thickness is not pronounced. As τ_{aer} increases, the dependence of relative difference on the azimuth viewing angle becomes somewhat stronger, especially, for $\delta_{0,h}$ and δ_h.

In all cases, the maximal error caused by the neglect of molecular absorption takes place for the multiple scattering component: $\delta_m > \delta$, $\delta_m > \delta_0$. At the same time, δ differs insignificantly from δ_0, and $\delta(\varphi)$ is close to linear $\delta(\varphi) \approx \delta_0(\varphi = 0)(1 + K\varphi)$: for example, for the solar almucantar $\delta(\varphi = 0) \approx \delta_0(\varphi = 0)$, and at $90 \le \varphi \le 180°$ $\delta(\varphi)$ and $\delta_0(\varphi)$ differ no more than 1.2 times. This fact may be practically useful. For example, to take molecular absorption into account when calculating the brightness field, it is possible to calculate first the sky brightness in the approximation of the aerosol atmosphere B^A by any acceptable procedure and then to introduce the correction for absorption by atmospheric gases, based on the data on δ_0, which characterizes the difference of brightness calculations for the single scattering component. We will demonstrate this by the example of the sky brightness in the almucantar. According to Eq. (12), the brightness $B^{AG} = B^A/(1 - \delta)$, and, as was noted above, δ can be presented as linearly depending on φ. Then, taking into account Eq. (15a), we finally obtain

$$B^{AG}(\varphi) \approx B^{A}(\varphi)/[1 - \delta_0(1 + K\varphi)] = \\ = B^{A}(\varphi)/[1 - (1 + K\varphi)\tau^{G}_{\Delta\lambda}(m)], \qquad (16)$$

where the coefficient K for all considered conditions varies slightly $K \approx (1.25 \pm 0.2) \cdot 10^{-3}$.

Table 2. Absolute Δ (μW · cm^{-2} · sr^{-1}) and relative δ (%) errors in calculation of diffuse radiation

λ, μm	Λ_{aer}	τ_{aer}	$\xi_\odot = 60°$				$\xi_\odot = 80°$			
			φ = 10°		φ = 90°		φ = 10°		φ = 90°	
			$-\Delta \cdot 10^{-8}$	−δ, %	$-\Delta \cdot 10^{-8}$	−δ, %	$-\Delta \cdot 10^{-8}$	−δ, %	$-\Delta \cdot 10^{-8}$	−δ, %
Solar almucantar (ξ = $\xi_\odot$)										
0.50	0.898	0.06	2.8	2.0	0.9	2.3	9.3	5.2	2.6	5.6
		0.4	7.7	1.9	1.4	2.2	9.2	5.1	1.8	5.3
0.87	0.840	0.03	2.5	2.8	0.3	3.1	8.5	4.2	0.9	4.4
		0.2	11.9	2.8	1.2	3.1	23.6	4.2	1.9	4.3
2.137	0.771	0.03	2.8	3.9	0.1	4.9	14.3	9.4	0.3	10.6
		0.1	8.6	4.0	0.3	4.8	35.5	9.4	1.0	10.6
1.245	0.781	0.03	5.5	7.3	0.5	8.6	28.9	18.2	1.8	19.8
		0.1	16.3	7.3	1.3	8.5	68.9	18.3	4.3	20.1
Horizon (ξ = 89°)										
0.50	0.898	0.06	8.3	3.0	2.9	3.3	16.1	6.0	2.8	6.3
		0.4	5.6	2.2	1.7	2.4	4.7	5.3	1.2	5.3
0.87	0.840	0.03	19.9	5.1	4.3	5.4	37.8	5.5	3.4	5.9
		0.2	20.0	4.0	3.9	4.1	23.8	4.7	2.3	4.7
2.137	0.771	0.03	25.9	17.2	3.7	18.0	90.1	20.3	3.0	21.3
		0.1	28.5	12.3	4.2	12.8	88.2	16.2	3.4	17.0
1.245	0.781	0.03	71.8	25.8	13.1	28.4	171.7	34.5	12.2	37.9
		0.1	71.9	17.7	12.7	18.4	159.7	27.4	11.6	28.3

N o t e . The spectral channels are presented in the increasing order of $\tau^{G}_{\Delta\lambda}(m)$, $A_s = 0.2$.

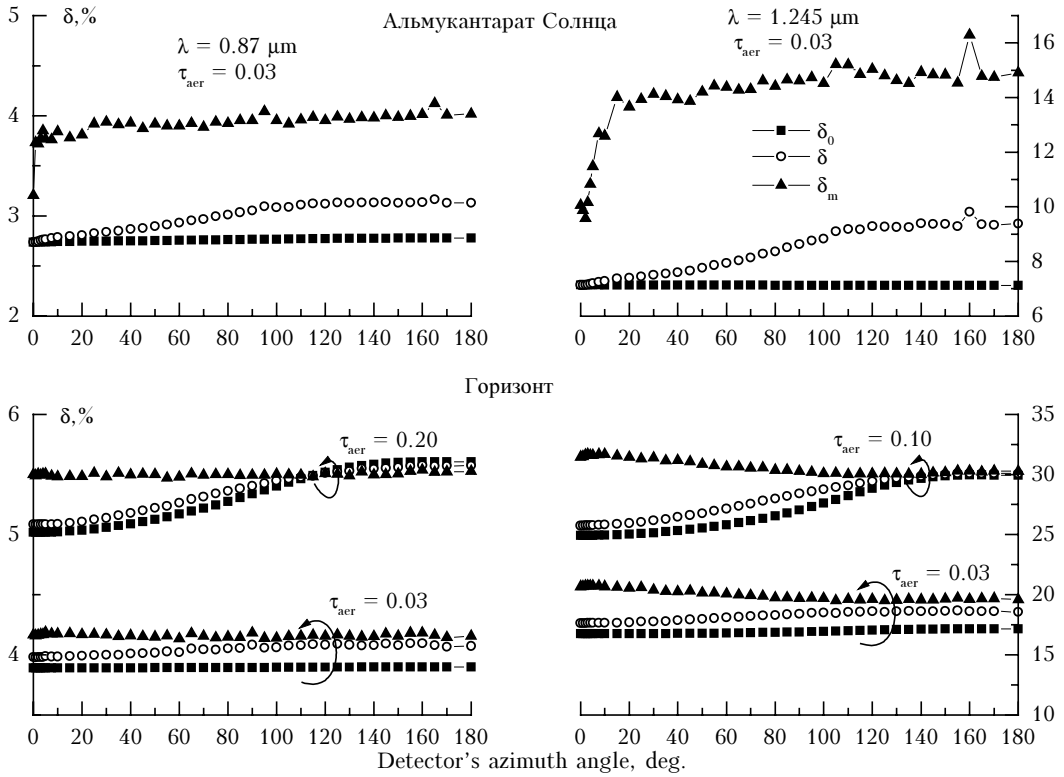

Fig. 4. Azimuth dependence of relative errors in brightness calculations for different spectral channels ($\xi_\odot = 60°$, $A_s = 0.2$).

4. Effect of aerosol

In the shortwave atmospheric transmission windows, main effect on the incoming radiation is due to aerosol. The angular dependence of the brightness single scattering component in the near-horizon zone of the sky $B^{AG}_{0,h}(\theta)$ is determined by the scattering phase function at the surface level $h = 0$ that accounts for the relative contribution of the aerosol $g_{aer}(\theta)$ and molecular $g_R(\theta)$ scattering phase functions (see Ref. 1):

$$g(\theta) = \frac{\sigma_{aer}(0)\Lambda_{aer}(0)}{\sigma_{aer}(0)\Lambda_{aer}(0) + \sigma_R(0)} g_{aer}(\theta) + \frac{\sigma_R(0)}{\sigma_{aer}(0)\Lambda_{aer}(0) + \sigma_R(0)} g_R(\theta),$$

where σ_{aer} and σ_R are the aerosol extinction and molecular scattering coefficients.

The multiple-scattered brightness component has qualitatively the same angular structure, but its dependence on $g(\theta)$ is more complex, and elongation of $B^{AG}_{m,h}(\theta)$ is not so significant as compared to $B^{AG}_0(\theta)$. For typical values of the aerosol optical thickness, the angular dependence of $B^{AG}_h(\theta)$ is mostly formed by $B^{AG}_{0,h}(\theta)$ (Fig. 5).

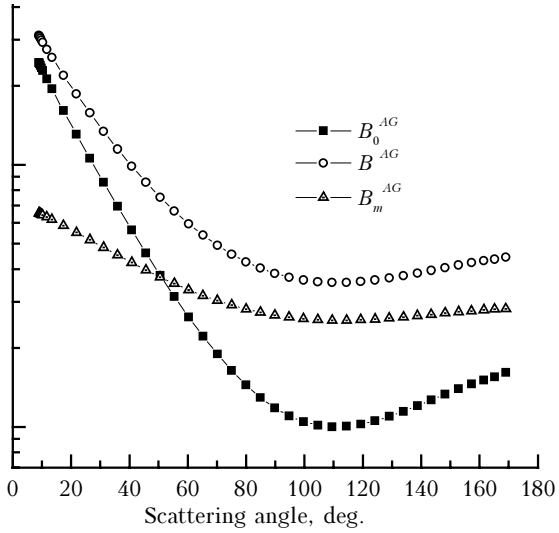

Fig. 5. Angular structure of brightness $B^{AG}_h(\varphi)$ and its single- $B^{AG}_{0,h}(\varphi)$ and multiple- $B^{AG}_{m,h}(\varphi)$ scattered components at $\tau_{aer} = 0.2$ and $\xi_\odot = 85°$.

The more detailed consideration of the regularities in formation of the brightness field near the horizon $B^{AG}_h(\xi, \varphi)$ will be presented in the third, final part of this paper, and here the consideration is restricted to discussion of the effect of the aerosol optical thickness and the single scattering albedo on the sky brightness in the 0.5 μm spectral interval taken as an example ($\tau_R = 0.146$; $A_s = 0.2$).

According to the radiative transfer theory, the dependence of the diffuse radiation on τ_{aer} in the atmosphere is affected by two factors. On the one hand, the increase of the aerosol optical thickness means the increase in the number of scatterers and, consequently, causes the increase of brightness. On the other hand, the increase of τ_{aer} leads to more significant extinction of radiation reaching an elementary scattering volume and, as a consequence, causes a decrease of the diffuse radiation. The competition of these two opposing factors may be the cause of deviation from the monotonic dependence of the sky brightness at increase of the aerosol optical thickness. The presence and the position of the maximum of sky brightness as functions of τ_{aer} are also determined by the geometry of the experiment and other optical characteristics of the atmosphere.

Figure 6 shows the calculated sky brightness near the horizon for typical values of the aerosol optical thickness and $\xi_\odot \geq 60°$.

At azimuth viewing angles $\varphi < 90°$, B^{AG}_h has the pronounced maximum, whose position shifts to the smaller τ_{aer} values as $\xi_\odot$ increases (Fig. 6*a*). At the increasing azimuth ($\varphi > 90°$) $B^{AG}_h(\tau_{aer})$ transforms into the monotonically decreasing function of τ_{aer} (Fig. 6*b*). The analysis of the results shows that at large $\xi_\odot \geq 75°$ and $\tau_{aer} \geq 0.05$ the brightness of the near-horizon sky area decreases with the increase of τ_{aer} in the entire range of viewing angles $0 \leq \varphi \leq 180°$ (Fig. 7).

Note that the nonmonotonic character of the dependence of $B^{AG}_h(\tau_{aer})$ is determined, first of all, by its single scattering component; the behavior of multiple scattering component is qualitatively similar, but its maximum is less pronounced and shifted to larger values of τ_{aer}.

In Ref. 1 we have shown that the effect of variations of the aerosol single scattering albedo at $h > 2$ km on $B^{AG}_h(\varphi)$ is negligibly small. Consider how the incoming radiation depends on Λ_{aer} in a denser near-surface layer $h < 2$ km.

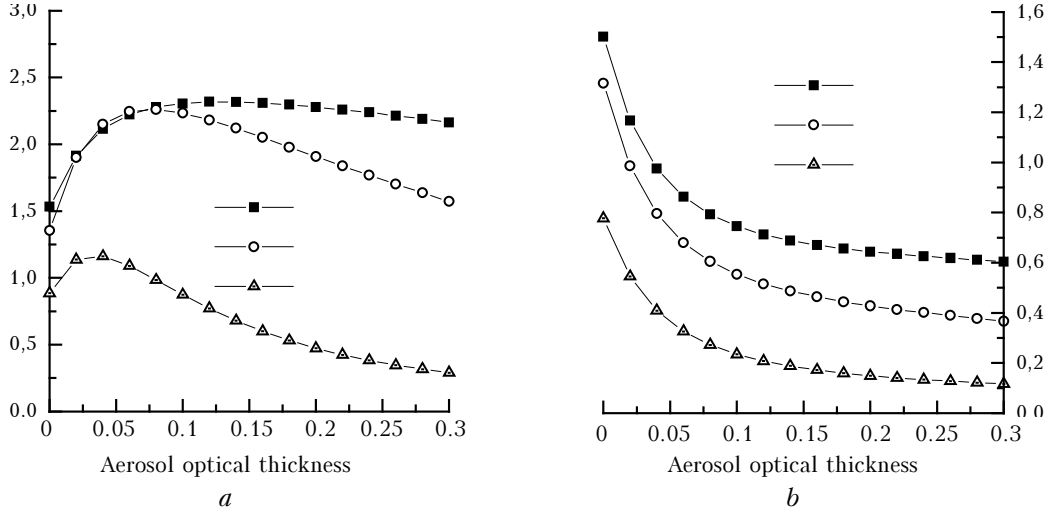

Fig. 6. Dependence of brightness near the horizon on the aerosol optical thickness for two detector's azimuth angles.

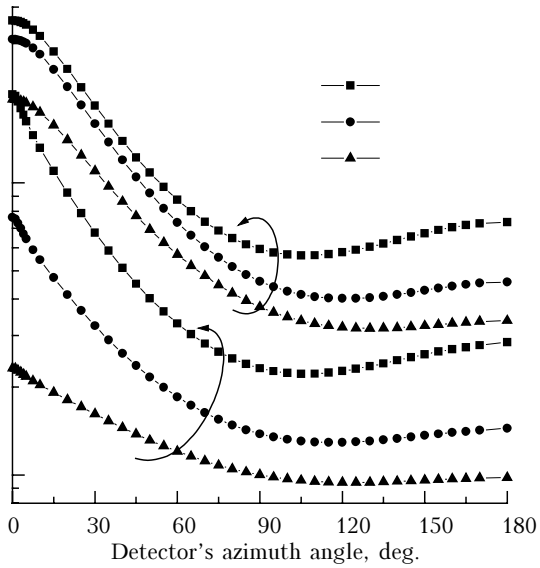

Fig. 7. The effect of aerosol optical thickness on the angular structure of brightness $B_h^{AG}(\varphi)$ at different zenith solar angles.

The analysis of the calculated results shows that, unlike the aerosol thickness, B_h^{AG} and its components have a simpler dependence on Λ_{aer}, which is characterized by practically linear decrease at decreasing Λ_{aer}. To understand the mechanism, through which Λ_{aer} affects the brightness field of the incoming radiation, consider how B_h^{AG}, $B_{0,h}^{AG}$, and $B_{m,h}^{AG}$ vary within the typical range $0.85 \le \Lambda_{aer} \le 1$ and $\tau_{aer} = 0.2$ (Fig. 8).

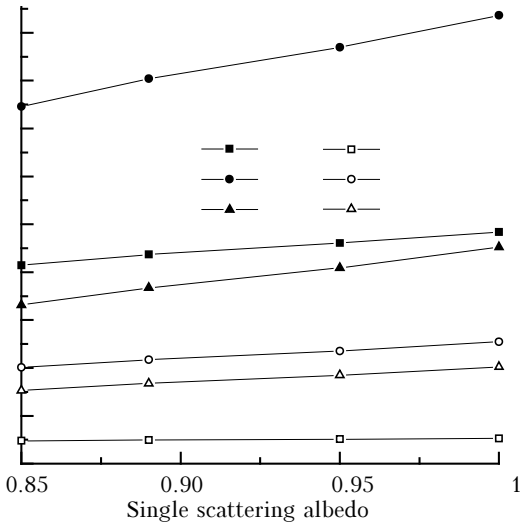

Fig. 8. Dependence of brightness on the aerosol single scattering albedo at $\tau_{aer} = 0.2$ and $\xi_\odot = 75°$.

The single-scattered brightness component is formed under the effect of the scattering phase function [Eq. (14)]:

1) in the forward direction of scattering ($\varphi = 30°$), aerosol has a dominant effect on $B_{0,h}^{AG}(\varphi)$, hence the ranges of variation of $B_{0,h}^{AG}(\varphi)$ and Λ_{aer} almost coincide (~ 17%);

2) at large azimuth angles ($\varphi = 150°$), the role of molecular scattering increases, and the effect of Λ_{aer} on $B_{0,h}^{AG}(\varphi)$ weakens (~ 10%).

The more significant dependence on Λ_{aer} is observed for the multiple scattering component of brightness because of the increase in the number of scattering and absorption events: the variations of $B_{m,h}^{AG}$ depending on φ are 30–36%. The increase in the aerosol absorptance within the indicated limits is accompanied by the 26–32% decrease in the sky brightness. It is important that variation of the solar zenith angle has almost no effect on the dependence of B_h^{AG} on Λ_{aer}.

Note that the considered regularities in formation of the sky brightness near the horizon also hold for other shortwave windows.

Conclusion

This paper presents the efficient algorithm for calculation of the diffuse solar radiation by the conjugate walk method in the spherical cloudless atmosphere. The molecular absorption and the spectral instrumental functions of photometers have been taken into account through the parameters of expansion of the transmission function into the exponential series.

With some typical examples (spectral ranges and atmospheric conditions) we have demonstrated the need of taking into account the absorption by atmospheric gases when calculating the sky brightness in atmospheric transmission windows at large zenith viewing angles. It has been shown that the neglect of molecular absorption gives relative errors $\delta = 2$–40% that depend mostly on the slant absorption optical thickness, and these errors increase as we pass on from solar almucantar measurements to the horizon measurements. The peculiarities in behavior of δ open the possibility of approximate consideration of molecular absorption in calculations of the brightness fields [for example, in the form of approximation (16) for the almucantar].

Using the 0.5 μm spectral channel as an example, we have considered the effect of aerosol on the sky brightness near the horizon. It has been shown that for the azimuth viewing angles $\varphi < 90°$ the dependence of the sky brightness on the aerosol thickness may be nonmonotonic with a maximum nearby $\tau_{aer} \approx 0.03$–0.15. This regularity can also be observed for some brightness components caused by the single and multiple scattering. The sky brightness in the rear hemisphere (with respect to the direction to the sun) monotonically decreases with increasing τ_{aer} for typical atmospheric conditions.

The dependence of the sky brightness near the horizon on the single scattering albedo is close to linear (the brightness increases with the increase of Λ_{aer}), and it has a stronger effect on the radiation caused by the multiple scattering. The effect of Λ_{aer} on the single-scattered brightness component is maximal near the solar vertical ($\varphi \to 0$), where the ranges of variation of brightness and Λ_{aer} coincide. At the increasing azimuth,

the dependence $B_h^{AG}(\Lambda_{aer})$ becomes weaker because of redistribution of contributions of aerosol and molecular scattering.

Acknowledgments

This work was partly supported by the Russian Foundation for Basic Research (Grant No. 02–05–64492) and DOE's ARM Program (Contract No. 5012).

References

1. T.B. Zhuravleva, I.M. Nasretdinov, and S.M. Sakerin, Atmos. Oceanic Opt. **16**, Nos. 5–6, 496–504 (2003).
2. G.Sh. Livshits, *Light Scattering in the Atmosphere* (Nauka, Alma-Ata, 1965), 177 pp.
3. O. Dubovik, B. Holben, Y. Kaufman, M. Yamasoe, A. Smirnov, D. Tanre, and I. Slutsker, J. Geophys. Res. D **103**, No. 24, 31903–31923 (1998).
4. K.M. Firsov, T.Yu. Chesnokova, V.V. Belov, A.B. Serebrennikov, and Yu.N. Ponomarev, Vychisl. Tekhnol. **7**, No. 5, 77–87 (2002).
5. J. of Geophys. Res. **96** (D5) (1991).
6. A.A. Mitsel', K.M. Firsov, and B.A. Fomin, *Transfer of Optical Radiation in the Molecular Atmosphere* (STT, Tomsk, 2001), 444 pp.
7. M. Chou and L. Kouvaris, J. Geophys. Res. D **96**, No. 5, 9003–9012 (1991).
8. Ph. Riviere, A. Soufani, and J. Taine, J. Quant. Spectrosc. Radiat. Transfer **48**, No. 2, 187–203 (1992).
9. D.M. Stam, P. Stammes, J.W. Hovenier, and J.F. de Haan, in: *Proc. of the International Radiation Symposium, IRS'96: Current Problems in Atmospheric Radiation* (Fairbanks, Alaska, 1996), pp. 830–833.
10. W. Armbruster and J. Fisher, Appl. Opt. **35**, No. 12, 1931–1941 (1996).
11. R.G. Ellingson, in: *Proc. of the Eighth Atmospheric Radiation Measurement (ARM) Science Team Meeting* (Tuscon, Arisona, 1998), pp. 245–248.
12. *A Preliminary Cloudless Standard Atmosphere for Radiation Computation. World Climate Research Programme*, WCP 112, WMO/TD No. 24 (1986), 60 pp.
13. G. Anderson, S. Clough, F. Kneizys, J. Chetwynd, and E. Shettle, *AFGL Atmospheric Constituent Profiles* (0–120 km), Air Force Geophysics Laboratory, AFGL-TR-86-0110, Environmental Research Paper No. 954 (1986).
14. E.V. Pyaskovskaya-Fesenkova, *Investigation of Light Scattering in the Earth's Atmosphere* (USSR Academy of Sciences Press, Moscow, 1957), 219 pp.
15. V.A. Smerkalov, *Applied Atmospheric Optics* (Gidrometeoizdat, St. Petersburg, 1997), 334 pp.